



# Combination of additive and subtractive laser 3D microprocessing in hybrid glass/polymer microsystems for chemical sensing applications

TITAS TIČKŪNAS,<sup>1</sup> MATTHIEU PERRENOUD,<sup>2</sup> SIMAS BUTKUS,<sup>1</sup>  
ROALDAS GADONAS,<sup>1</sup> SIMA REKŠTYTĖ,<sup>1</sup> MANGIRDAS  
MALINAUSKAS,<sup>1</sup> DOMAS PAIPULAS,<sup>1,\*</sup> YVES BELLOUARD,<sup>2,3</sup> AND  
VALDAS SIRUTKAITIS<sup>1</sup>

<sup>1</sup>Vilnius University, Faculty of Physics, Laser Research Center, Sauletekio Ave. 10, LT-10223 Vilnius, Lithuania

<sup>2</sup>Ecole Polytechnique Fédérale de Lausanne (EPFL), Galatea Lab, STI/IMT, Rue de la Maladière 71b, CH-2002 Neuchâtel, Switzerland

<sup>3</sup>yves.bellouard@epfl.ch

\*domas.paipulas@ff.vu.lt;

**Abstract:** We present a novel hybrid glass-polymer micromechanical sensor by combining two femtosecond laser direct writing processes: laser illumination followed by chemical etching of glass and two-photon polymerization. This incorporation of techniques demonstrates the capability of combining mechanical deformable devices made of silica with an integrated polymer structure for passive chemical sensing application. We demonstrate that such a sensor could be utilized for investigating the elastic properties of polymeric microstructures fabricated via the two-photon polymerization technique. Moreover, we show that polymeric microstructure stiffness increases when immersed in organic liquids.

© 2017 Optical Society of America

**OCIS codes:** (140.3390) Laser materials processing; (140.7090) Ultrafast lasers; (350.3850) Materials processing (160.5470) Polymers; (160.6030) Silica; (230.4000) Microstructure fabrication.

## References and links

1. Y. Kondo, J. Qiu, T. Mitsuyu, K. Hirao, and T. Yoko, "Three-dimensional microdrilling of glass by multiphoton process and chemical etching," *Jpn. J. Appl. Phys.* **38**, L1146 (1999).
2. A. Marcinkevičius, S. Juodkazis, M. Watanabe, M. Miwa, S. Matsuo, H. Misawa, and J. Nishii, "Femtosecond laser-assisted three-dimensional microfabrication in silica," *Opt. Lett.* **26**, 277–279 (2001).
3. Y. Bellouard, A. Said, M. Dugan, and P. Bado, "Fabrication of high-aspect ratio, micro-fluidic channels and tunnels using femtosecond laser pulses and chemical etching," *Opt. Express* **12**, 2120–2129 (2004).
4. K. Sugioka, J. Xu, D. Wu, Y. Hanada, Z. Wang, Y. Cheng, and K. Midorikawa, "Femtosecond laser 3D micromachining: a powerful tool for the fabrication of microfluidic, optofluidic, and electrofluidic devices based on glass," *Lab Chip* **14**, 3447–3458 (2014).
5. S. Maruo, O. Nakamura, and S. Kawata, "Three-dimensional microfabrication with two-photon-absorbed photopolymerization," *Opt. Lett.* **22**, 132–134 (1997).
6. J. Serbin, A. Egbert, A. Ostendorf, B. Chichkov, R. Houbertz, G. Domann, J. Schulz, C. Cronauer, L. Frohlich, and M. Popall, "Femtosecond laser-induced two-photon polymerization of inorganic-organic hybrid materials for applications in photonics," *Opt. Lett.* **28**, 301–303 (2003).
7. M. Malinauskas, A. Žukauskas, S. Hasegawa, Y. Hayasaki, V. Mizeikis, R. Buividas, and S. Juodkazis, "Ultrafast laser processing of materials: from science to industry," *Light Sci. Appl.* **5**, e16133 (2016).
8. S. Kiyama, S. Matsuo, S. Hashimoto, and Y. Morihira, "Examination of etching agent and etching mechanism on femtosecond laser microfabrication of channels inside vitreous silica substrates," *J. Phys. Chem. C* **113**, 11560–11566 (2009).
9. D. Tan, Y. Li, F. Qi, H. Yang, Q. Gong, X. Dong, and X. Duan, "Reduction in feature size of two-photon polymerization using SCR500," *Appl. Phys. Lett.* **90**, 071106 (2007).
10. L. Amato, Y. Gu, N. Bellini, S. Eaton, G. Cerullo, and R. Osellame, "Integrated three-dimensional filter separates nanoscale from microscale elements in a microfluidic chip," *Lab Chip* **12**, 1135–1142 (2012).
11. D. Wu, S.-Z. Wu, J. Xu, L.-G. Niu, K. Midorikawa, and K. Sugioka, "Hybrid femtosecond laser microfabrication to achieve true 3D glass/polymer composite biochips with multiscale features and high performance: the concept of ship-in-a-bottle biochip," *Laser Photon. Rev.* **8**, 458–467 (2014).

12. D. Wu, J. Xu, L.-G. Niu, S.-Z. Wu, K. Midorikawa, and K. Sugioka, "In-channel integration of designable microoptical devices using flat scaffold-supported femtosecond-laser microfabrication for coupling-free optofluidic cell counting," *Light Sci. Appl.* **4**, e228 (2015).
  13. M. Olsen, G. Hjorto, M. Hansen, O. Met, I. Svane, and N. Larsen, "In-chip fabrication of free-form 3D constructs for directed cell migration analysis," *Lab Chip* **13**, 4800–4809 (2013).
  14. J. Xu, H. Kawano, W. Liu, Y. Hanada, P. Lu, A. Miyawaki, K. Midorikawa, and K. Sugioka, "Controllable alignment of elongated microorganisms in 3D microspace using electrofluidic devices manufactured by hybrid femtosecond laser microfabrication," *Microsyst. Nanoeng.* **3**, 16078 (2017).
  15. A. Ovsianikov, X. Shizhou, M. Farsari, M. Vamvakaki, C. Fotakis, and B. N. Chichkov, "Shrinkage of microstructures produced by two-photon polymerization of Zr-based hybrid photosensitive materials," *Opt. Express* **17**, 2143–2148 (2009).
  16. H. Sun, T. Suwa, K. Takada, R. Zaccaria, M. Kim, K. Lee, and S. Kawata, "Shape precompensation in two-photon laser nanowriting of photonic lattices," *Appl. Phys. Lett.* **85**, 3708–3710 (2004).
  17. Q. Sun, K. Ueno, and H. Misawa, "In situ investigation of the shrinkage of photopolymerized micro/nanostructures: the effect of the drying process," *Opt. Lett.* **37**, 710–712 (2012).
  18. K. Takada, D. Wu, Q.-D. Chen, S. Shoji, H. Xia, S. Kawata, and H.-B. Sun, "Size-dependent behaviors of femtosecond laser-prototyped polymer micronanowires," *Opt. Lett.* **34**, 566–568 (2009).
  19. S. M. Kuebler, A. Narayanan, D. E. Karas, and K. M. Wilburn, "Low-distortion surface functionalization of polymeric microstructures," *Macromol. Chem. Phys.* **215**, 1533–1542 (2014).
  20. S. Reškštytė, D. Paipulas, M. Malinauskas, and V. Mizeikis, "Microactuation and sensing using reversible deformations of laser-written polymeric structures," *Nanotechnology* **28**, 124001 (2017).
  21. Y. Li, H. Cui, F. Qi, H. Yang, and Q. Gong, "Uniform suspended nanorods fabricated by bidirectional scanning via two-photon photopolymerization," *Nanotechnology* **19**, 375304 (2008).
  22. Q. Sun, S. Juodkazis, N. Murazawa, V. Mizeikis, and H. Misawa, "Freestanding and movable photonic microstructures fabricated by photopolymerization with femtosecond laser pulses," *J. Micromech. Microeng.* **20**, 035004 (2010).
  23. T. Ikegami, M. P. Stocker, K. Monaco, J. T. Fourkas, and S. Maruo, "Fabrication of three-dimensional metalized movable microstructures by the combination of two-photon microfabrication and electroless plating," *Jpn. J. Appl. Phys.* **51**, 6S (2012).
  24. H. Xia, J. Wang, Y. Tian, Q.-D. Chen, X.-B. Du, Y.-L. Zhang, Y. He, and H.-B. Sun, "Ferrofluids for fabrication of remotely controllable micro-nanomachines by two-photon polymerization," *Adv. Mater.* **22**, 3204–3207 (2010).
  25. P. Danilevičius, S. Reškštytė, R. Gadonas, M. Malinauskas, E. Balčiūnas, R. Jarašienė, D. Baltruikienė, V. Bukelskienė, A. Kraniuskas, and R. Širmenis, "Micro-structured polymer scaffolds fabricated by direct laser writing for tissue engineering," *J. Biomed. Opt.* **17**, 081405 (2012).
  26. H.-B. Sun, K. Takada, and S. Kawata, "Elastic force analysis of functional polymer submicron oscillators," *Appl. Phys. Lett.* **79**, 3173–3175 (2001).
  27. S. Nakanishi, S. Shoji, S. Kawata, and H.-B. Sun, "Giant elasticity of photopolymer nanowires," *Appl. Phys. Lett.* **91**, 063112 (2007).
  28. Z. Bayindir, Y. Sun, M. J. Naughton, C. N. LaFratta, T. Baldacchini, J. T. Fourkas, J. Stewart, B. E. A. Saleh, and M. C. Teich, "Polymer microcantilevers fabricated via multiphoton absorption polymerization," *Appl. Phys. Lett.* **86**, 064105 (2005).
  29. T. Baldacchini, V. Nuñez, C. N. LaFratta, J. S. Grech, V. I. Vullev, and R. Zadayan, "Microfabrication of three-dimensional filters for liposome extrusion," *Proc. SPIE* **9353**, 93530W (2015).
  30. C. N. LaFratta and T. Baldacchini, "Two-photon polymerization metrology: Characterization methods of mechanisms and microstructures," *Micromachines* **8**, 101 (2017).
  31. A. Žukauskas, I. Matulaitienė, D. Paipulas, G. Niaura, M. Malinauskas, and R. Gadonas, "Tuning the refractive index in 3D direct laser writing lithography: towards GRIN microoptics," *Laser Photon. Rev.* **9**, 706–712 (2015).
  32. Y. Bellouard, A. A. Said, and P. Bado, "Integrating optics and micro-mechanics in a single substrate: a step toward monolithic integration in fused silica," *Opt. Express* **13**, 6635–6644 (2005).
  33. Y. Bellouard, "On the bending strength of fused silica flexures fabricated by ultrafast lasers [Invited]," *Opt. Mater. Express* **1**, 816–831 (2011).
  34. A. Ovsianikov, J. Viertel, B. Chichkov, M. Oubaha, B. MacCraith, I. Sakellari, A. Giakoumaki, D. Gray, M. Vamvakaki, M. Farsari, and C. Fotakis, "Ultra-low shrinkage hybrid photosensitive material for two-photon polymerization microfabrication," *ACS Nano* **2**, 2257–2262 (2008).
  35. A. Skarmoutsou, G. Lolas, C. A. Charitidis, M. Chatzinikolaïdou, M. Vamvakaki, and M. Farsari, "Nanomechanical properties of hybrid coatings for bone tissue engineering," *J. Mech. Behav. Biomed.* **25**, 48–62 (2013).
  36. W. Xiong, Y. Liu, L. Jiang, Y. Zhou, D. Li, L. Jiang, J.-F. Silvain, and Y. Lu, "Laser-directed assembly of aligned carbon nanotubes in three dimensions for multifunctional device fabrication," *Adv. Mat.* **28**, 2002–2009 (2016).
  37. S. Reškštytė, T. Jonavičius, D. Gailevičius, M. Malinauskas, V. Mizeikis, E. Gamaly, and S. Juodkazis, "Nanoscale precision of 3D polymerization via polarization control," *Adv. Opt. Mater.* **4**, 1209–1214 (2016).
-

## 1. Introduction

Femtosecond laser pulses have enabled high precision fabrication of 3D structures in glass by subtractive laser-assisted etching (LAE) [1–4] as well as additive fabrication of polymers via two-photon polymerization (2PP) [5–7]. Due to their high-peak intensities, tightly focused femtosecond laser beams can trigger non-linear two-photon or multi-photon absorption phenomena. This unique characteristic leads to a modification of transparent material only within the focal point of laser beam. By spatially moving the laser focus, well-defined 3D patterns can be written. In the LAE technique glass is structurally modified so that laser affected zones are etched significantly faster than unaffected ones. This is observed in both HF [2] and KOH [8]. This technique allows for processing mm-cubes volumes or more with yet, micron resolution. Glass material provides robustness, transparency and biocompatibility to the structures [4].

Contrary to LAE, 2PP is an additive technique, which is based on the structuring of a photosensitive polymer, when polymerization reactions occurs at the focus point of the laser beam [5]. 2PP technique provides stretchable, but at the same time soft, complex-shape polymeric structures with a feature size resolution as small as few tens of nanometers [9]. Recently, novel device concepts were unraveled as 2PP technique was employed for additively incorporating functional 3D polymeric components in glass micro-voids/-channels [10].

Although, LAE and 2PP techniques exhibit different advantages and drawbacks, the combined use of subtractive and additive techniques open new possibilities for the fabrication of microstructures whose manufacturing was difficult or inaccessible using only one of the two techniques individually. New applications and functionalities could be achieved with such hybrid fabrication method for creating microfluidic devices for cell sorting, counting, liquid mixing and filtering applications [10–14].

An important feature of 2PP-made structures is that, during the development and drying processes, there is always a change in material state. On one hand, the polymerized material becomes denser and consequently geometrical structure dimensions turn out inevitably smaller than expected. This irreversible volume reduction is an effect of dissolution of the non-polymerized internal nanometer size pores of the structure [15–17]. On the other hand, polymeric structures can also swell after rinsing in solvents after (or during) developing process [18–20]. Strongly wetting solvents tend to penetrate the nanometric pores washed out by the developer so that polymeric structure expands. Although these phenomena have been investigated in a number of articles, most of the studies have been done only qualitatively and within a range of one to several tens of micrometers [17, 21, 22]. Furthermore, shrinkage and swelling phenomena have a potential to be applied in chemical sensing applications [20].

2PP-formed microstructures are also used in applications in the fields of microelectromechanics (MEMS) [23, 24] and bioengineering [25], where knowledge of the mechanical and elastic properties of a structure is essential. Several studies have investigated the elastic behavior of microstructures made with the 2PP technique: Sun *et al.* used optical tweezers to deflect polymeric micro-springs [26, 27], while others applied distance-force probing with a commercial atomic force microscope [28] or MEMS based force sensing probes [29] (a recent review on this topic can be found in reference [30]). These studies indicate that laser fabricated microstructures have lower stiffness if compared to the bulk polymer, due to inhomogeneous (voxel-to-voxel) polymerization [28], while in some cases giant elasticity (extreme low stiffness/shear module values) was reported [27]. Permeation of organic liquids in the polymer or scaling effects were considered as plausible causes for such unexpected behavior [27]. The wide range of factors that can contribute to microstructure elasticity makes this topic particularly challenging to investigate, but the emerging attractive applications that rely on elastic properties require detailed investigation.

In this article, to further improve hybrid manufacturing technology we present a coupled device concept consisting of LAE fabrication of a cantilever out of fused silica substrate with

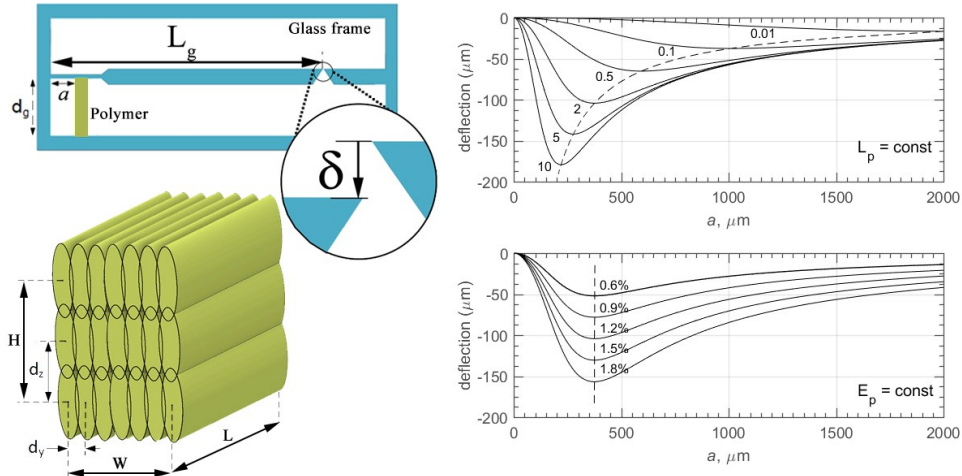


Fig. 1. (*top-left*) Sketch of the glass cantilever with integrated polymeric beam that may induce cantilever deflection due to the shrinkage/swelling effects. (*bottom-left*) A schematic construction of a polymer beam fabricated by LAE and 2PP methods. (*right*) Modeled cantilever tip deflection values versus distance along the cantilever where the polymer is integrated. Top graphs are modeled with a constant polymer shrinkage value (in this case 1.2% from original design value ( $d_g$ )) and a different Young's modulus (in GPa), while the bottom graph depicts a situation where the Young's modulus is constant (2 GPa) and shrinkage value is varied. Dashed curves depict maximum deflection trends in both graphs.

the direct integration of a polymeric beam via the 2PP technique. Through this combination of techniques, we demonstrate a novel hybrid glass-polymer micromechanical sensor used to investigate the elastic properties of polymeric microstructures. The well-defined geometry of the fused silica cantilever acts as an amplification system and tester for the quantitative investigation of the polymeric beam properties. In this context, we present the polymeric beam length change due to the shrinkage/swelling phenomena, as well as the Young's modulus estimation results of the SZ2080 polymer in different ambient surroundings, giving new insights into the behavior of the polymeric microstructures.

## 2. Cantilever design and theoretical model

The glass cantilever with the integrated polymeric beam is depicted in Fig. 1. The polymeric structure links the fixed glass base to the cantilever. Upon shrinkage or swelling, the beam shrinks or expands causing the cantilever to bend upwards or downwards. In a first approximation, this system can be analyzed as a cantilever beam with a point load. As the elastic properties of fused silica are well known, and considering the fact that silica is inert in most chemicals, the cantilever deflection allows for evaluating the reaction force applied on the polymer and in turn, for estimating its elastic properties.

Based on the assumption formulated above, the magnitude of the cantilever tip deflection ( $\delta$ ) is expressed as follows:

$$\delta = \frac{E_p S_p (L_p - d_g)(3L_g - a)a^2}{2(E_p S_p a^3 + 3E_g I_g L_p)}; \quad (1)$$

where  $E_g$  is the fused silica Young's modulus (72 GPa),  $L_g$  – the total cantilever length (10 mm),  $d_g$  – the distance between the cantilever and the glass base (342  $\mu\text{m}$ ),  $a$  – the distance between

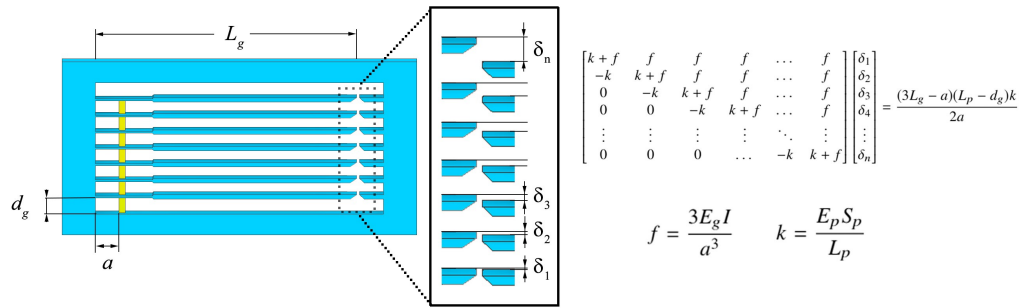


Fig. 2. A sketch of a coupled cantilever system consisting of several cantilevers interlinked with the polymer beam (each polymer segment is identical). A linear system equation that can be used to compute deflection of each cantilever is also included.

the fixed cantilever end and the polymer,  $I_g$  is the silica's second moment of inertia, (which for a rectangular cross-section is  $I_g = \frac{t_g w_g^3}{12}$ , with  $w_g$  – the cantilever width (35  $\mu\text{m}$ ), and  $t_g$  – its thickness (480  $\mu\text{m}$ )). The polymer cross-section is denoted by  $S_p$  (50  $\mu\text{m} \times 50 \mu\text{m}$ ).

Two parameters remain unknown:  $E_p$  – the Young's modulus of the polymer, and  $L_p$  – the final length of the polymer after swelling or shrinkage in the absence of a reaction force. These parameters can be estimated using a set of cantilevers in which the polymer beams are attached at different positions,  $a$  (see Fig.1). Shifting the polymer beam attachment point scales the reaction force and allows for probing the polymer elasticity under fixed conditions and polymer beam length. Figure 1 (right) shows typical plots of cantilever deflection with different polymer elasticity. One can see that the shrinkage/swelling of the polymer (change in  $L_p$  value) influences only the overall magnitude of deflection, while a change in  $E_p$  shifts the maximum deflection position along the cantilever beam. Therefore, it is possible to unambiguously fit the data to both unknown parameters using Eq. (1). As we will see later, both parameters are environmentally dependent and can be utilized for chemical sensing applications.

The modulus of elasticity is a material property, while the stiffness ( $k$ ) describes elasticity of a structure made from the material in question. In our case the polymeric structure is a rectangular beam made by direct laser writing (DLW) with a dense patterning algorithm. Although, the structure is made by combining discrete patterns, we assume it is dense enough, so that it is reasonable to consider it as a plain and homogeneous beam of Young modulus  $E_p$ . If necessary  $E_p$  could be interchanged with  $k$  in Eq. (1) using Young's modulus expression as  $E_p = \frac{kL_p}{S_p}$ .

A slightly different cantilever sensor can be designed by linking several identical cantilevers into one combined system as shown in Fig. 2. Here, each cantilever's reaction force applies to all polymeric segments that are below the cantilever, therefore in each segment different force scaling is achieved allowing for probing the polymer elasticity. To compute each cantilever deflection, one needs to solve the linear system equation depicted in Fig. 2. As in Eq. (1), there are two unknown parameters:  $E_p$  and  $L_p$ . The benefit of such a system lies in its simpler polymeric beam integration procedure, as the polymeric beam can be recorded in one single step (simultaneously through all cantilevers), automatically making all segments identical in term of geometry and exposure parameters, an increase in repeatability can be expected. The main drawback is the reduced lack of accuracy, because polymeric segments close to the glass base experiences a higher glass stiffness resulting in greater reaction forces that considerably reduces the cantilever deflections, making it hard to measure (optimizing the sensor design by making each cantilever of different thickness can overcome this problem). This design was created as a substitute for the

simple cantilever model if sufficient polymeric integration repeatability could not be achieved in the former case. It turned out that repeatability was not a problem; therefore we used the coupled cantilever design as an alternative method to estimate polymeric elastic properties.

### 3. Experimental details

The glass processing and polymer integration experiments were conducted using a DLW method employing a single Yb:KGW femtosecond laser system (Pharos, Light Conversion). The sample was translated using dual XY linear stages (ANT130-XY, Aerotech Inc.), while the laser focus spot was changed using a vertical Z stage (ANT160L-Z, Aerotech Inc.).

The monolithic glass cantilevers were produced from a single piece of 500  $\mu\text{m}$ -thick fused silica substrate by combining femtosecond laser radiation and subsequent chemical etching. Glass modifications were induced with laser beam having circular polarization at 1030 nm laser wavelength, using 270 mW laser power (rep. rate 610 kHz), while focusing with 0.4 NA objective. Laser pulse duration was increased to 600 fs in order to achieve better etching selectivity. The multiple laser-modified tracks along the predefined cantilever perimeter were recorded at 15 mm/s velocity in layer-by-layer fashion with 4.5  $\mu\text{m}$  spacing.

After laser exposure, the fused silica substrate was immersed in a low-concentration 5% (v/v) hydrofluoric acid (HF) solution for 6 hours. Cantilevers were later rinsed in distilled water and afterwards dried. Using this method several cantilevers were made close to each other in one monolithic glass block.

Afterwards, the fabricated cantilever structure was put on a standard microscope cover glass and fully covered with photosensitive polymer using the drop-casting method. For this experiment we used a hybrid inorganic/organic photosensitive polymer SZ2080, which was additionally photo-sensitized with 1% wt of 2-benzyl-2-(dimethylamino)-4'-morpholinobutyrophenone photoinitiator. SZ2080 polymer immersed in glass cantilevers was firstly prebaked for 1.5 h on a hot-plate with a temperature ramp of 40°C – 90°C.

The 2PP experiments were carried out using a frequency-doubled wavelength (515 nm) at 200 fs-width pulses operated at a 610 kHz repetition rate. The specimen was loaded on the same XY linear stage system, but using a tighter focusing objective (0.8 NA). A polymeric rectangular-shape beam was integrated in the glass structure (top surface of the polymer was 10  $\mu\text{m}$  below the glass surface level). The total size of the polymeric beam was ( $H \times W \times L = 50 \times 50 \times 342$ )  $\mu\text{m}^3$ , while two different pattern densities were used: one (I) with parameters  $dy = 0.25$   $\mu\text{m}$  and  $dz = 1.5$   $\mu\text{m}$  while the other (II) with  $dy = 0.5$   $\mu\text{m}$  and  $dz = 4.5$   $\mu\text{m}$  (see Fig. 1). In both cases the voxels overlap in all three dimensions, forming a continuously polymerized structure. However in the first case the total exposure dose is higher allowing for a higher degree of conversion of monomers, which impacts polymer swelling properties [20, 31]. In both hatching cases, an average power of 0.8 mW was used and the writing velocity was 3 mm/s. To scale the cantilever reaction force, polymeric microbeams were integrated at different positions from the cantilever base and, in each configuration, three equal polymer-cantilever systems were fabricated in order to test the experiment's repeatability. After 2PP processing, the samples were immersed in a developer bath (4-methyl-2-pentanone (PEN)) for 20 – 30 min to wash out unexposed material.

The glass cantilever based on previous work on glass flexures [32, 33] has low stiffness in one plane while remaining stiff for out-of-the-plane movement. By immersing such a composite micromechanical system in various liquids or allowing the sample to dry (a critical point dryer K850 (Quorum Technologies) was used for drying specimens), a polymer swelling/shrinkage phenomenon occurs, causing the cantilever beam to deform through bending. The composite micromechanical cantilever system was immersed in different liquids (PEN, ethanol and water), which resulted in different cantilever deflection angles, demonstrating the sensing mechanism.

#### 4. Results and discussion

The fabricated cantilever with integrated polymer beam is shown in Fig. 3. The polymeric beam fabricated in high pattern density condition (I), as discussed in the previous paragraph, undergoes shrinkage right after development as can be seen from the cantilever deflection data depicted in Fig. 4. Initially, the deflection is measured when the sensor is still in the developer (PEN), which later is interchanged with ethanol. Afterwards, the liquids are evaporated and the deflection is measured in air. The evaporation has to be carried out in a critical point drying condition, in order to prevent capillary forces from acting on the glass cantilever, resulting in polymer breakage or detachment of the polymeric beam from the glass substrate. In all cases the data were fitted using the least square method applied to the Eq. (1). As can be seen, there is a good fit of the experimental data with the theoretical model. The fitting parameters ( $E_p$ ,  $L_p$ ) are as follows: immersed in PEN: ( $0.188 \pm 0.005$  GPa;  $339.5 \pm 0.1$   $\mu\text{m}$ ); ethanol: ( $0.158 \pm 0.007$  GPa;  $339.6 \pm 0.1$   $\mu\text{m}$ ) and air: ( $0.138 \pm 0.008$  GPa;  $340.1 \pm 0.1$   $\mu\text{m}$ ). Fitting errors are within the 95% confidence interval (dashed curves in figures). Note that the possible cantilever geometry estimation errors are not present in the fitted data (all cantilevers are identical), and are not important if comparative analysis between three different environments is carried out. If one includes geometrical measurement errors (i.e. assuming 5% precision in measuring all cantilever dimensions), the absolute values for Young's modulus and shrinkage/swelling can be estimated with  $\sim 25\%$  precision (evaluated by Monte Carlo simulation) by this method.

The results show that the average polymer shrinkage is about 0.6 %. This value is expected as SZ2080 is considered as an ultra-low shrinkage photosensitive polymer [15, 34]. However there is an evident increase in the Young's modulus when the polymeric beam is immersed in the organic liquid. The cantilever reaction force builds up due to the increased polymer stiffness and not to the polymer shrinkage.

A similar tendency is present in samples made with the lower density (II) scheme. In these cases, the samples swell as high affinity (strongly wetting) solvents such as PEN or ethanol penetrate the internal nanoscale pores causing the polymer to expand. In contrast, water or other low affinity solvents empty the pores causing the polymers to shrink [20].

The cantilever deflection curves are shown in Fig. 5(a), and fitted values are as follow: PEN ( $0.467 \pm 0.018$  GPa;  $345.8 \pm 0.1$   $\mu\text{m}$ ) and ethanol ( $0.493 \pm 0.015$  GPa;  $345.1 \pm 0.1$   $\mu\text{m}$ ). Samples were also tested in water, but the cantilever did not show any deflection, suggesting that shrinkage/swelling is too low to induce sufficient forces (for the same reason sample drying was not attempted in this case). Remarkably, these results indicate an increase of up to 3 times in the Young's modulus if compared to the higher density patterning scheme. Internal presence of organic liquid molecules in the polymer network considerably increases its stiffness and makes

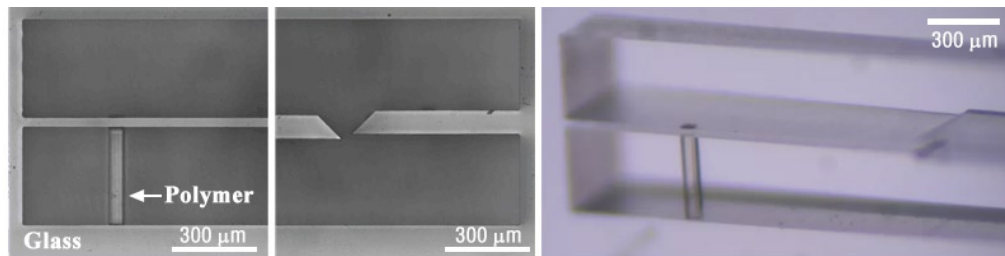


Fig. 3. Fused silica cantilever with SZ2080 polymeric beam fabricated by the hybrid femtosecond laser processing technique. The optical microscope images indicate the deflection of the cantilever after polymer shrunk in air. The picture on the right shows a stereoscopic microscope image of a hybrid sensor.

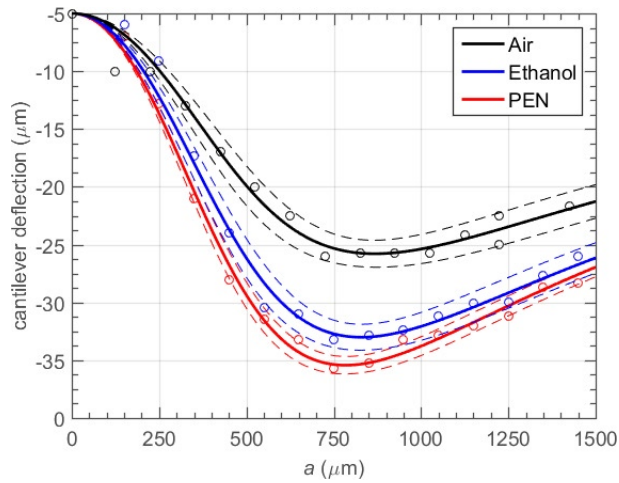


Fig. 4. Cantilever deflection induced by polymer shrinkage in various organic liquids and air.

cantilever actuation stronger. Additionally, the swelling behavior is reversible and repeatable. Figure 5(b) depicts the cantilever deflection change when the sample is periodically immersed in different liquids. Even after 10 cycles of ethanol–PEN changes, the deflection magnitude remained the same. This also applies to water–organic solvent cycles, when deflection changes are maximized. This fact makes such hybrid micromechanical systems attractive for chemical sensing applications.

Similar values for polymer elastic properties were acquired with the coupled cantilever system, as shown in Fig.6. The least square fit of the model gives slightly lower Young's modulus values than in the previous case, but taking into account absolute 25 % precision the values match in both experiments.

Our study shows that the Young's modulus in 2PP fabricated structures differ by an order of magnitude from typical values for bulk SZ2080 polymer hardened by continuous UV radiation [35]. A similar trend was observed in other laser-polymerized photosensitive resins such as SR369 [29] and SR499/368 [28]. On the contrary, Sun *et al.* reported much lower stiffness values when a sample is immersed in organic liquid [26,27]. Solvent permeation into the polymer was speculated

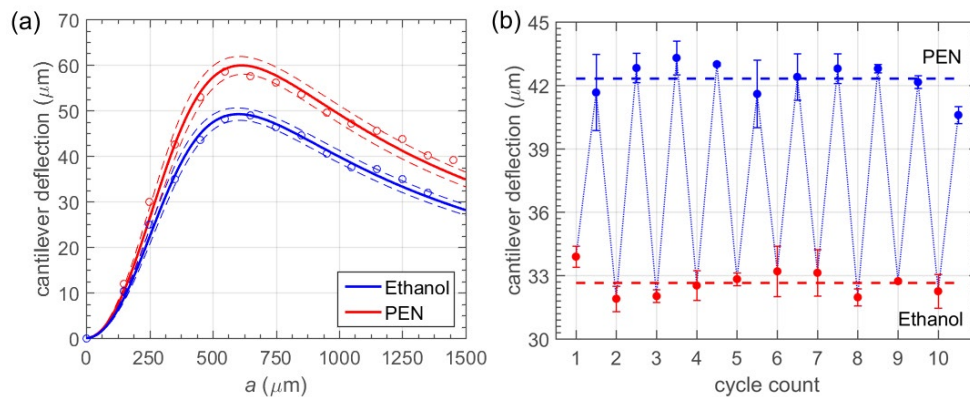


Fig. 5. (a) Cantilever deflection induced by polymer swelling in organic liquids. (b) Cantilever deflection dependence on the solvent change cycle number.

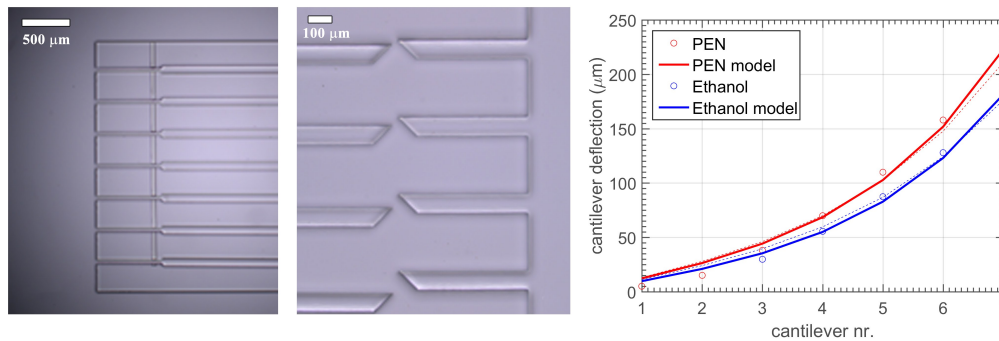


Fig. 6. The manufactured cantilever system, consisting of seven interlinked cantilevers. Microscope images are shown on the *left* and *center* (cantilevers are immersed in PEN). (*right*) Deflection of the coupled system in different solvents: solid curves show the least square fit of the data computed from the coupled cantilever model (Fig. 2), fit parameters: PEN (0.40 GPa, 346.4  $\mu\text{m}$ ) and ethanol (0.389 GPa, 345.6  $\mu\text{m}$ ); dashed curves show the model fit with parameters evaluated from the single cantilever experiment (Fig. 5(a)).

as one of the possible causes for a drop in the polymer elasticity. In our research, we show that organic solvent increases the polymer stiffness, especially in those cases where the degrees of conversion were lower. These contradicting results can be attributed to different polymer type and/or scaling effects.

## 5. Conclusions

In summary, we have demonstrated a novel hybrid glass-polymer micromechanical sensor that can be utilized for investigating the elastic properties of polymeric microstructures fabricated by the 2PP technique. The results indicate that the 2PP made microstructures of hybrid organic-material can vary in mechanical properties depending on the surrounding solvent. In most cases there is an evident increase in Young's modulus while the structure is submerged in organic liquids. Some further studies could be conducted to reveal the influence of the direct laser writing scanning trajectory [36], exposure conditions – including dose, voxel overlap, and considering polarization for final 3D microstructures mechanical properties [37]. The change in Young's modulus can be utilized for chemical sensing applications as shown with our glass cantilever setup.

## Funding

Swiss-Lithuanian Institution Cooperation Programme “Research and Development” (Grant No. CH-3-ŠMM-02/05).

## Acknowledgment

The Galatea Lab at EPFL acknowledges the sponsoring of Richemont International.